ELSEVIER

Colloids and Surfaces A: Physicochem. Eng. Aspects 211 (2002) 233–248

COLLOIDS AND SURFACES A

www.elsevier.com/locate/colsurfa

A quantitative comparison between chemical dosing and electrocoagulation

Peter K. Holt [a], Geoffrey W. Barton [a,*], Mary Wark [a], Cynthia A. Mitchell [b]

[a] *Department of Chemical Engineering, University of Sydney, Sydney, NSW 2006, Australia*
[b] *Institute for Sustainable Futures, University of Technology Sydney, PO Box 123 Broadway, Sydney NSW 2007, Australia*

Received 9 November 2001; accepted 12 June 2002

Abstract

A renewed interest in electrocoagulation has been spurred by the search for reliable, cost-effective water treatment processes. This technology delivers the coagulant in situ as the sacrifcial anode corrodes, due to an applied potential, while the simultaneous evolution of hydrogen at the cathode allows for pollutant removal by flotation. By comparison, conventional chemical dosing typically adds a salt of the coagulant, with settling providing the primary pollutant removal path. This paper provides a quantitative comparison of these two approaches based on turbidity removal associated with a clay pollutant. Chemical coagulation was evaluated via jar tests using aluminium sulphate (alum). This proved more effective than electrocoagulation under acidic conditions (pH $\sim$4) and low coagulant levels (4 mg-Al l^{-1} being the minimum able to effectively destabilise the colloidal clay particles). Highly effective coagulation was observed at intermediate alum dosage levels (4–20 mg-Al l^{-1}), where the isoelectric point occurred at pH $\sim$7.8. Three operating stages (lag, reactive and stable) were identified in a batch electrocoagulation reactor with the operating current determining the pollutant removal rate. At the isoelectric point, which occurs during the reactive stage, the greatest turbidity reduction occurs, indicating aggregation by a sorption mechanism (compared to the charge neutralisation as in the case of chemical coagulation). During the stable stage, continued precipitation of aluminium hydroxide and a decrease in turbidity indicated a sweep coagulation mechanism. The highest current (2 A) reduced the pollutant level in the shortest time, 1% residual turbidity after 30 min, though the highest efficiency (in terms of pollutant removed per unit of aluminium added) was achieved at the lowest current (0.25 A).

Keywords: Electrocoagulation; Alum dosing; Water treatment; Electrochemical; Aluminium electrodes

1. Introduction

1.1. Historical perspective

Electrocoagulation is currently experiencing a renaissance. At the turn of the nineteenth century, it was seen as a promising technology, in fact, a

* Corresponding author. Tel.: +61-29351-3780; fax: +61-29351-2854
E-mail address: barton@chem.eng.usyd.edu.au (G.W. Barton).

0927-7757/02/$ - see front matter
PII: S0927-7757(02)00285-6

water treatment plant was successfully commissioned in London at this time [1]. In the following decades, plants were also commissioned in the United States to treat municipal wastewater. By the 1930s, however, all such plants had been abandoned due to perceived higher operating costs [2] and the ready availability of mass-produced alternatives for chemical coagulant dosing.

In recent years, however, smaller scale electrocoagulation processes have found a niche in the water treatment industry, proving to be reliable and effective technologies [1–7], though requiring greater technical understanding for their potential to be fully exploited. Only recently has research aimed at a quantitative understanding of electrocoagulation's relatively complex pollutant removal mechanisms [3].

1.1.1. Chemical coagulation

The stability of a pollutant is determined by its physicochemical properties. Many pollutants are composed of similarly charged particles that repel each other, with the repulsive forces creating a stable, colloidal system. In order to maintain electroneutrality, oppositely charged ions, typically hydroxyl (OH^-) or hydrogen ions (H^+), are attracted to the (charged) pollutant particles. The attraction of counter ions to a negatively charged pollutant forms an electric double layer divided into a Stern and diffuse layer [8–11]. It is difficult to measure the charge at the colloid surface, due to the charge concentrations in the Stern and diffuse layers [8]. Consequently, the zeta potential is used as an experimental measure of the 'effective' charge of the particle as it moves through the solution, thus providing a direct indicator of solution stability [11].

Electrostatic repulsion between electric double layers drives particles apart, whilst van der Waals forces act to bring them together. The interaction between these forces of attraction and repulsion can be described by the Deryaguin and Landau, Verwey and Overbeek (DLVO) theory [12,13]. The energetics are such that attraction dominates at small separations. However, to arrive at small separations, a repulsive energy barrier must first be overcome.

The coagulant's role here is to destabilise the colloidal suspension by reducing the attractive forces, thereby lowering the energy barrier and enabling particles to aggregate. A number of coagulation mechanisms including charge neutralisation, double layer compression, bridging and sweep, have been postulated dependent on the physical and chemical properties of the solution, pollutant and coagulant [9,11,14].

1.1.2. Coagulation by metal cations

Metal salt coagulants are commonly used in water treatment and in this study aluminium sulphate ($Al_2(SO_4)_3 \cdot 18H_2O$) is used as the chemical coagulant. Aluminium is also frequently used as the sacrificial anode in an electrocoagulation reactor. In both cases, chemical dosing and electrocoagulation, the metal cation hydrolyses upon addition to solution. Mononuclear complexes are initially formed as described by Eqs. (1)–(4).

$$Al^{3+} + H_2O \rightarrow AlOH^{2+} + H^+ \quad (1)$$

$$AlOH^{2+} + H_2O \rightarrow Al(OH)_2^+ + H^+ \quad (2)$$

$$Al(OH)_2^+ + H_2O \rightarrow Al(OH)_3^0 + H^+ \quad (3)$$

$$Al(OH)_3^0 + H_2O \rightarrow Al(OH)_4^- + H^+ \quad (4)$$

The extent of hydrolysis depends upon total metal concentration and pH, as well as the amount of other species present in solution. Fig. 1 is the solubility diagram for aluminium hydroxide, $Al(OH)_3(s)$, assuming only mononuclear species [data by Spositio, 15]. The solubility boundary denotes the thermodynamic equilibrium that exists between the dominant aluminium species at a given pH and solid aluminium hydroxide. The minimum solubility, 0.03 mg-Al l^{-1}, occurs at pH 6.3, with solubility increasing as the solution becomes more acidic or alkaline [11,16,17].

However, as the aluminium concentration increases and/or the solution 'ages', polynuclear aluminium complexes are formed and aluminium hydroxide precipitates, as shown below.

$$Al^{3+} \rightarrow Al(OH)_n^{(3-n)} \rightarrow Al_2(OH)_2^{4+} \rightarrow Al_{13}\ \text{complex} \rightarrow Al(OH)_3 \quad (5)$$

The speciation of aluminium systems has been well documented in the literature [15,18], although

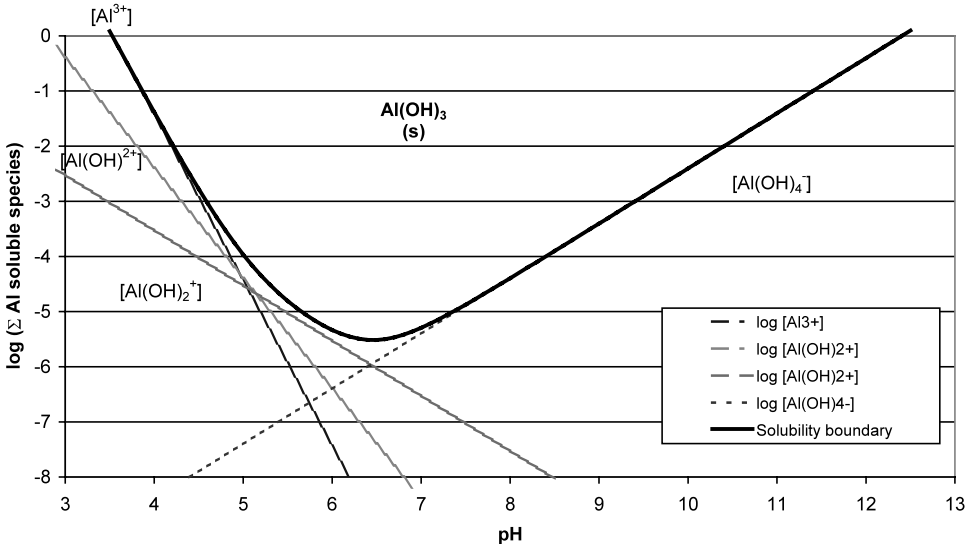

Fig. 1. Solubility diagram of aluminium hydroxide $Al(OH)_3(s)$ considering only mononuclear aluminium species.

little information is available on the kinetics that determines the rate at which thermodynamic equilibrium is attained. The complexity of the aqua-aluminium system is neither completely understood nor completely quantified [16,17]. This paper will assume mononuclear hydrolysed species adequately predict aluminium hydroxide precipitation.

1.2. Electrocoagulation

Electrocoagulation is a complex process, with a multitude of mechanisms operating synergistically to remove pollutants from the water. A wide variety of opinions exist in the literature for both the key mechanisms and the best reactor configurations. Design variations include a fluidised-bed reactor employing aluminium pellets [4], bipolar aluminium electrodes [5], mesh electrodes [1], as well as simple plate electrodes [2,6]. There is certainly no dominant 'electrocoagulation reactor' in use. Reported operating conditions and performance mirror the wide variation in design, with reactors invariably being 'tuned' to best suit a specific application. These empirical approaches invariably prove the viability of the technology, but singularly fails to fully capitalise on its potential. This is due to a lack of fundamental understanding of the system and hence the inability to accurately predict performance.

Fig. 2 begins to show the complex, interdependent nature of the electrocoagulation process [3,7]. A sacrificial metal anode (usually aluminium, but sometimes iron) is used to dose polluted water with a coagulating agent [1–7]. Simultaneously, electrolytic gases (mainly hydrogen at the cathode) are generated.

It is possible to identify three separate categories of mechanistic processes — electrochemistry, coagulation, and hydrodynamics — that form the basis of electrocoagulation. The fact that these processes are difficult to investigate separately in an operational reactor goes some way towards explaining the lack of a detailed technical literature on electrocoagulation.

1.3. Present study

Chemical dosing delivers the coagulant as a salt that dissociates in solution with hydrolysis of the aluminium cation (and associated anions) determining solution speciation and pH. Alum addition, for example, acidifies the water. By contrast, aluminium added via electrocoagulation does not bring with it any associated salt anions, with the result that the pH typically stabilises in the alka-

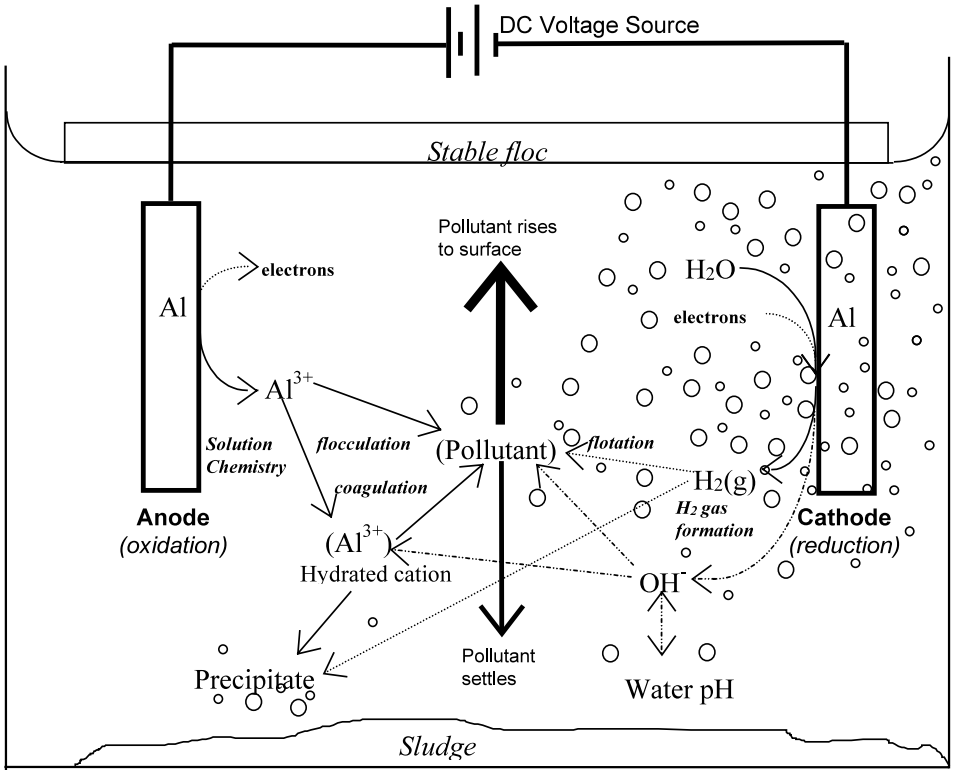

Fig. 2. Interactions occurring within an electrocoagulation reactor.

line range. The fact that electrolytic gases are also being produced has also been seen as an unnecessary complication [5]. Alternatively, these gases can be seen as being beneficial to the separation process. The coagulant's delivery and its nature influence the coagulation and separation processes by its speciation, removal path and associated by-products (salt anions for chemical coagulation and electrolytic gases for electrocoagulation).

Although electrocoagulation is seen as a promising technology, there is a perception that it is simply chemical dosing by another name, with the only difference being the way in which the coagulant is delivered. The objective in this paper is to quantitatively compare chemical dosing and electrocoagulation to determine dominant coagulation mechanisms and separation processes. The two approaches were evaluated by monitoring key solution characteristics (such as coagulant level, pH and zeta potential) in a series of chemical dosing jar tests and electrocoagulation runs carried out in a 7 l batch reactor.

2. Experimental method

2.1. Chemical coagulation experiments

Chemical coagulation was evaluated using an adaptation of the standard jar testing technique [19], with AR grade (99.8% pure) aluminium sulphate as the chemical coagulant. Sodium hydroxide and hydrochloric acid solutions were added for any subsequent pH adjustment. The pollutant used was a 'potter's clay', comprising kaolinite (67%), quartz (25%), illite/mica (3%), feldspar (3%) and other trace elements (2%), as characterised by X-ray diffraction analysis.

A concentrated aluminium sulphate solution (1 mg-Al ml^{-1}) was added to a clay mixture

(at 1 g l^{-1}), the mixture rapidly mixed (at more than 140 rpm) for a period of 30 s, with the solution then left to settle [20]. No further mixing occurred. In the runs carried out, the initial clay concentration was always at 1 g l^{-1}, while aluminium sulphate and pH were varied. Once rapid mixing had ceased (this being defined as time zero), samples were taken at 0, 1, 3, 5, 10, 15, 20, 25, 30, 45 and 60 min. Turbidity, zeta potential and pH were then measured off-line using a Merck Turbiquant 1500T (tungsten lamp), Malvern Zetasizer and a calibrated pH meter, respectively. All experiments were conducted at ambient temperature (nominally 20 °C).

2.2. Electrocoagulation experiments

The batch electrocoagulation reactor used (see Fig. 3) is constructed of perspex and has a maximum capacity of 7.1 l. The pollutant used here was the same batch of potter's clay described above. Fig. 4 is a schematic diagram of the electrode arrangement; five stainless steel cathodes are interspersed with four aluminium anodes, with brass rods used to connect the parallel plate electrodes.

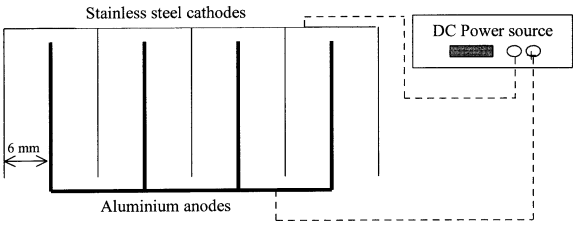

Fig. 4. Schematic diagram of electrode arrangement.

Electrical conductivity, total dissolved solids (TDS), salinity and temperature were all measured using a WTW LF340 probe, while pH was measured in a flow-through cell drawing solution from the reactor at a rate of 0.30 l min^{-1} using a peristaltic pump. The current flowing through the cell and the voltage across the electrodes were both recorded using a data logger. The current was held constant for each run. Current was investigated over the range 0.25–2.0 A. Aluminium concentration was measured using a Varian Atomic Absorption Spectrophotometer. Again, turbidity and zeta potential were measured off-line using a Merck Turbiquant 1500T (tungsten lamp) and Malvern Zetasizer.

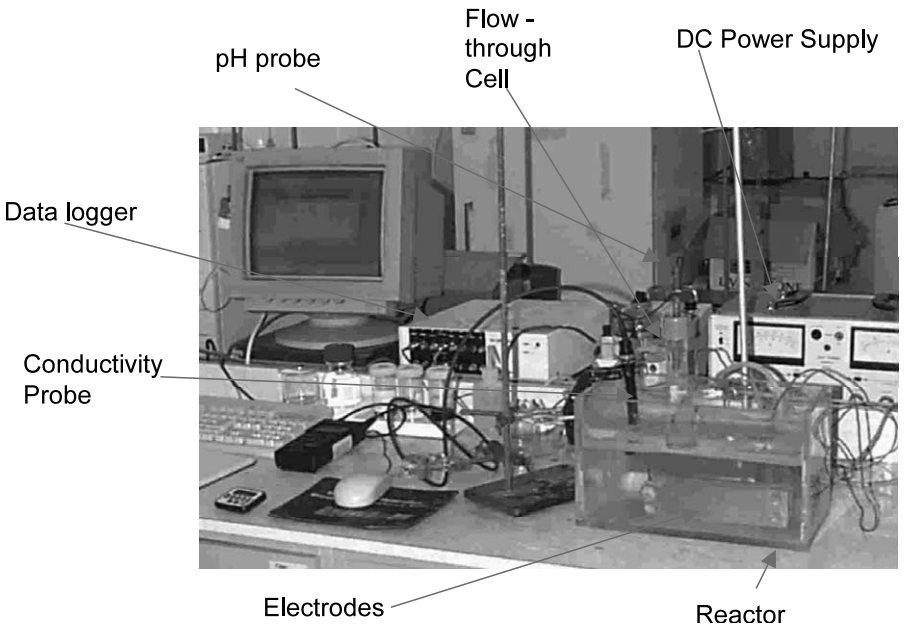

Fig. 3. Experimental electrocoagulation reactor.

All electrocoagulation experiments were conducted under standard conditions, that is, initial clay pollutant loading was always 1.0 g l^{-1}, in 6 l of de-ionised water, with 200 mg l^{-1} sodium chloride to enhance conductivity.

3. Results and discussion

Three broad aluminium concentration ranges — low (less than 4 mg-Al l^{-1}), medium (4–40 mg-Al l^{-1}) and high (greater than 40 mg-Al l^{-1}) — were used as a basis for comparing the effectiveness of chemical dosing and electrocoagulation at equivalent aluminium concentrations.

3.1. Clay removal

3.1.1. During chemical dosing

Normalised turbidity values as a function of settling time, that is, since the cessation of rapid mixing, for the dosage range 0–200 mg-Al l^{-1} studied are presented in Fig. 5. Intermediate aluminium concentrations (4–40 mg-Al l^{-1}) produced effective and very similar turbidity reduction profiles. Overdosing (i.e. 200 mg-Al l^{-1}) or underdosing (<4 mg-Al l^{-1}) produced less effective turbidity removal. Poor coagulation performance at low alum concentrations (0 and 2 mg-Al l^{-1}) suggests insufficient coagulant for pollutant destabilisastion. At the highest alum dosage tested (200 mg-Al l^{-1}), turbidity removal was less effective than at lower dosages, most likely indicating some measure of colloidal restabilisation was occurring [17].

The pH for these runs was monitored but not controlled. In these jar tests; the initial pH was 5.5 with the pH decreasing rapidly upon alum addition. At an alum dosage level of 4 mg-Al l^{-1}, the final pH was 4.4, while at 200 mg-Al l^{-1} the pH was 3.6. Alum dosing acidifies the solution, with the pH dropping as the dosage level increases.

3.1.2. During electrocoagulation experiments

Fig. 6 is a semi-log plot showing the normalised turbidity and pH profiles for a typical electrocoagulation run, where the initial clay concentration was 1.0 g l^{-1}, and the operating current was kept constant at 0.5 A. Three stages can clearly be identified-namely, a lag, a reactive and a stabilising stage. Little or no turbidity change is observed in the lag, with the majority ($\sim$95%) of turbidity removal occurring during the reactive stage. As time progresses, the rate of turbidity reduction decreases, with the turbidity eventually levelling out above zero. The pH stabilised to 8.5 after 10

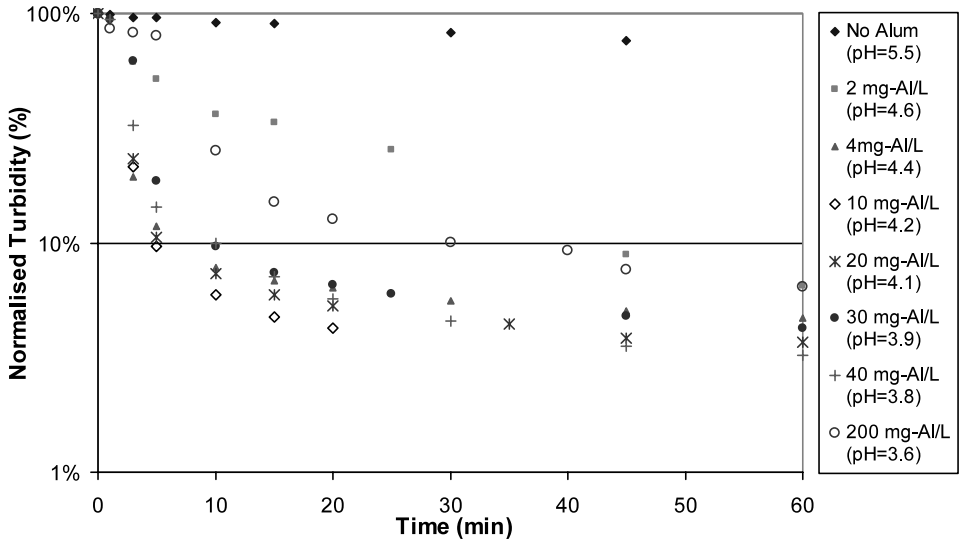

Fig. 5. Normalised turbidity for 1 g l^{-1} clay solutions as a function of time and chemical dosing level.

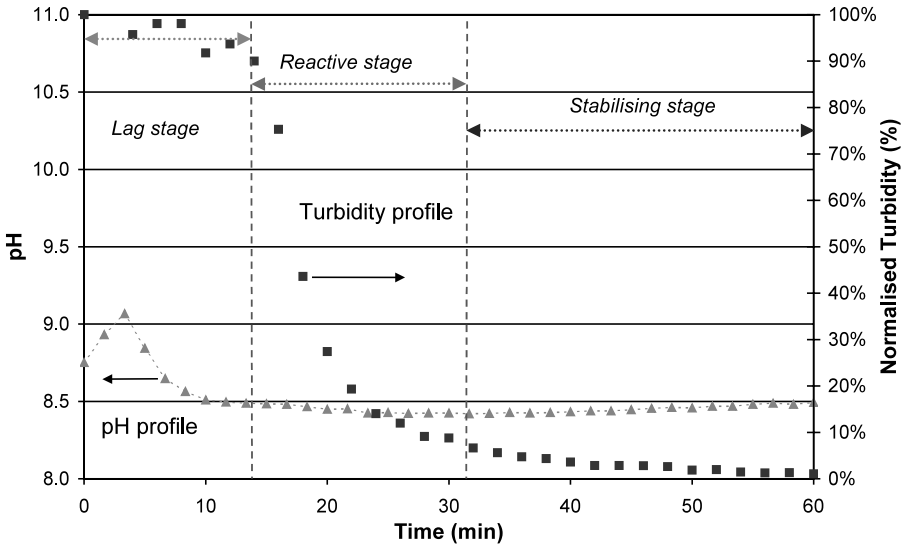

Fig. 6. Normalised turbidity and pH for 1 g l^{-1} clay solution subjected to electrocoagulation at a constant current of 0.5 A.

min of applied current. Note that while the system pH was monitored, it was not controlled, thus, the stabilisation of the pH is a characteristic of the electrocoagulation reactor.

For this clay pollutant, batch electrocoagulation approaches a stable alkaline pH, which might be taken as implying stable speciation within the solution. Yet the process is inherently dynamic, with aluminium entering the system, being hydrolysed in a complex manner and being removed from the system. Simultaneously water is being reduced adding hydroxyl ions into solution. Such dynamic changes in concentration affect both the solution speciation and the equilibrium state towards which the system is moving at any one time. Although jar tests (using alum) may also be seen as a time-varying process, the dynamics (to a first approximation) might be regarded as less severe, with coagulant addition occurring just once, and thus the system moving towards just one equilibrium state.

The important point here is that in a jar test the coagulant addition is a discrete event, with the system behaving as a (shot-fed) batch reactor moving towards a defined final equilibrium state. The (non-continuous flow) electrocoagulation reactor behaves more like a fed-batch system with coagulant being added continuously, at a rate dependent on electrode/solution properties and the applied current. As a result, the equilibrium towards which such a reactor is moving, is itself constantly shifting. These differences in dynamic behaviour contribute significantly to the distinction between chemical dosing and electrocoagulation.

3.2. Zeta Potential measurements

As previously discussed, colloids are maintained in suspension by electrostatic repulsion between particles. The zeta potential provides an effective measurement of the charge on a particle. Addition of aluminium coagulant can suppress the electric double layer around colloidal particles, thus encouraging aggregation of the pollutant [11].

3.2.1. Zeta potential for chemical dosing

Fig. 7 shows the zeta potential of clay at low alum concentrations (0, 2 and 4 mg-Al l^{-1}) for pH adjusted from 3–11. The colloidal clay system (with no alum addition) is stable, with the particles being negatively charged. Alum addition (to 2 and 4 mg-Al l^{-1}) increased the zeta potential, although it remained below zero. At these concentrations, there is insufficient coagulant to effectively reduce the pollutant's electric double layer to enable

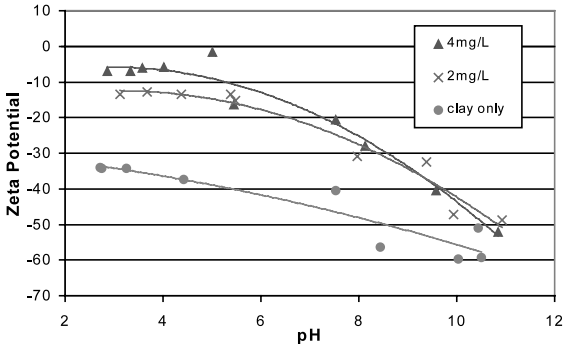

Fig. 7. Zeta potential for 1 g l^{-1} clay solutions subjected to chemical dosing at 0, 2 and 4 mg-Al l^{-1} of alum.

destabilisation. The ineffective destabilisation is reflected by the sub-optimal turbidity removal at 0 and 2 mg-Al l^{-1} alum (Fig. 5). At an alum concentration of 4 mg-Al l^{-1}, particles approached the isoelectric point and coagulation performance improved markedly (also see Fig. 7). Generally, the zeta potential decreased with increasing pH. This is probably due to an increase in negatively charged ions, specifically the hydroxyl ion added to increase the pH, and the aluminate ion, $Al(OH)_4^-$ (aq), which is dominant above pH ~9 [11,17].

At intermediate alum concentrations (10 and 20 mg-Al l^{-1}), the zeta potential increases from −3.5 mV at low pH values, to a maximum of + 14.5 mV at pH ~5.1, before decreasing as the solution becomes more alkaline. Fig. 8 shows that the suspension passes through two isoelectric points at approximate pH values of 4.0 and 7.8.

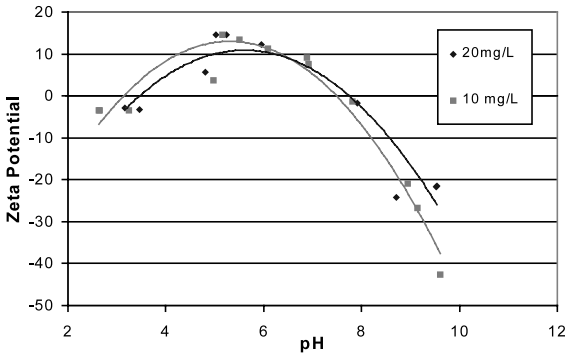

Fig. 8. Zeta potential for 1 g l^{-1} clay solution subjected to chemical dosing at 10 and 20 mg-Al l^{-1} of alum.

Effective turbidity removal is observed at pH 4.1–4.2 which corresponds to the isoelectric point (see Fig. 5). At this pH, the highly charged aluminium(III) cation, Al^{3+}(aq), is the dominant species [11,15] that binds to the negatively charged clay pollutant. Thus the solution is destabilised by a charge neutralisation mechanism at alum concentrations of 10 and 20 mg-Al l^{-1}.

3.2.2. Zeta potential for electrocoagulation

Fig. 9 presents the zeta potential measurements for the electrocoagulation reactor as a function of time for an applied current of 0.5 A, along with normalised turbidity measurements relative to the initial value. Initially, there is no change observed in the zeta potential — a response that mirrors the lag stage in the reactor. As the amount of coagulant dissolved at the anode increases, a point is reached where there is a sudden decrease in turbidity and the zeta potential increases rapidly, passing through the isoelectric point. The pH stabilises to 8.5 before the reactive stage and its profile is presented in Fig. 6. As the run progresses, turbidity, zeta potential and pH stabilise.

The beginning of the reactive stage may be defined as the point where a rapid decrease in turbidity commences. Fig. 9 shows that the isoelectric point occurs during this reactive stage. This isoelectric point occurs at pH 8.5 which is comparable to results obtained from chemical coagulation with the occurrence of an isoelectric point at pH ~8 (see Fig. 8). Assuming mononuclear aluminium speciation, the aluminate ion, $Al(OH)_4^-$(aq), is the dominant specie at pH 8.5. The negatively charged clay could not be destabilised by a negative aluminium ion hence coagulation by charge neutralisation appears implausible. Nevertheless, the aluminium solution chemistry model has assumed the presence of mononuclear species only. Extension of this model (using Outokumpu HSC Chemistry's thermodynamic package) to include polynuclear species, specifically the aluminium tri-meric specie, $Al_3(OH)_4^{5+}$(aq), shifts the pH from 6.6 to 10.7. This pH range spans the region of interest thus suggesting that this highly charged positive ion might be responsible for destabilisation and coagulation. Regardless, the overlap, that is the correspondence of the iso-

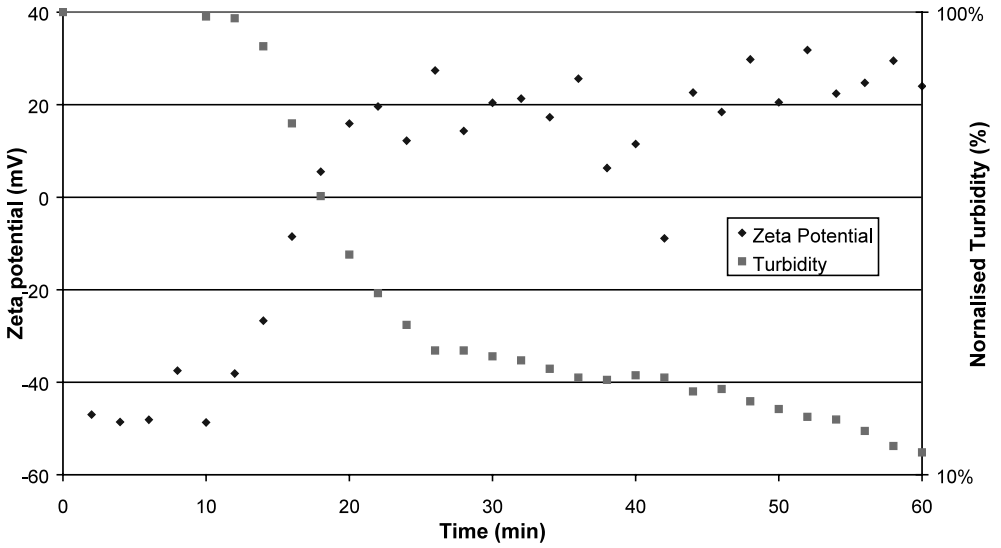

Fig. 9. Zeta potential for 1 g l^{-1} clay solution subjected to electrocoagulation at a constant current of 0.5 A.

electric point and the rapid turbidity reduction, together with the nature of the aluminium coagulant and clay pollutant, strongly suggests that some type of sorption mechanism is the primary coagulation mechanism here [11,17].

As the system moves into the stable stage, the rate of turbidity reduction continues to decrease, while the zeta potential increases above the isoelectric point before stabilising (see Fig. 9). Increase in zeta potential indicates re-stabilisation of the solution, thus a sorption coagulation mechanism is not possible during the stable stage. At pH range of interest, 8.3–8.8, thermodynamics predicts precipitation of aluminium hydroxide when total aluminium concentration exceeds 2.1–6.7 mg-Al l^{-1}, respectively (Fig. 1). This data, together with the fact that aluminium continues to be added to solution and hydrolysed with aluminium hydroxide precipitating, would seem to indicate a gradual shift to sweep flocculation (or enmeshment) as the dominant pollutant removal mechanism in the stable stage. The residual turbidity levels were explored by operating the electrocoagulation reactor with and without clay present.

Fig. 10 presents the normalised turbidity within the electrocoagulation reactor, both with pollutant initial clay loading of 1 g l^{-1} and without clay. The interesting point to note is the increase during the reactive stage in turbidity level over time when no clay is present. In this scenario the only solution changes are due to the dissolution of the aluminium anode and the cathodic reduction of water so this turbidity increase is best explained by the production of a precipitate. During the stabilising stage, turbidity levels converged. This would seem to suggest that the residual turbidity observed in electrocoagulation runs with clay is due to the electrocoagulation process and not the clay. That is, the turbidity rise in the 'no pollutant' case representing the establishment of a steady-state between the production and flotation of hydrolysed aluminium hydroxide flocs. This hypothesis is further explored by measurements of total aluminium both in solution and as a precipitate, with and without clay. These results are shown in Fig. 11. Faraday's law is used to relate the current flow (I for time t) to the amounts (m) of aluminium and hydroxide ions generated within the reactor, and hence provides a theoretical amount for total aluminium.

$$m = \frac{I \times t \times M}{ZF} \tag{6}$$

Z is the number of electrons transferred in the reaction at the electrode, M is the molecular

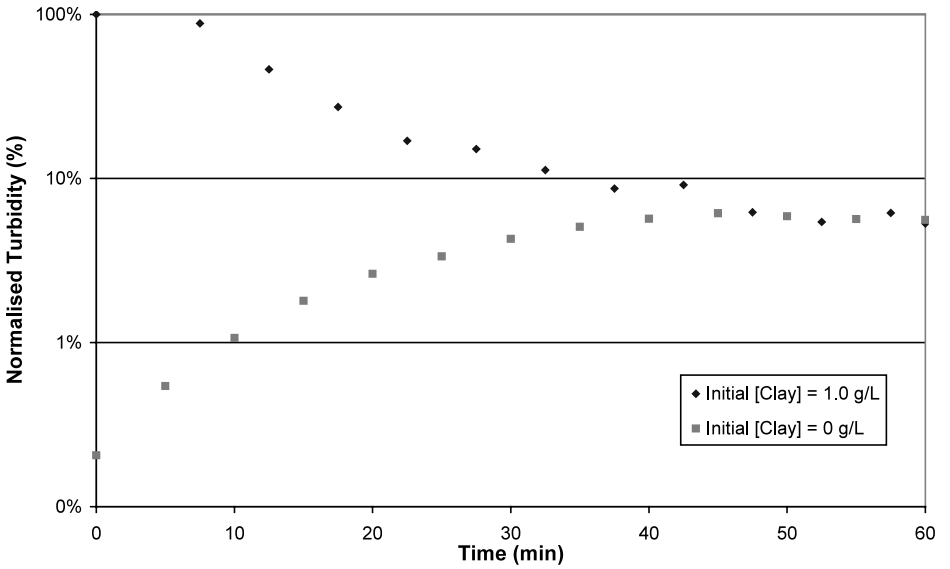

Fig. 10. Normalised turbidity for 1 and 0 g l^{-1} clay solution subjected to electrocoagulation at a constant current of 1.0 A.

weight (g mol^{-1}) and F is Faraday's constant (96 486 C mol^{-1}).

Measured total aluminium concentration for runs with and without clay remained below that predicted by Faraday's law (as shown in Fig. 11). When clay is present, the total aluminium concentration was consistently below 5 mg l^{-1}. The bulk of the coagulant must be bound to the clay pollutant and hence removed with the pollutant. This observation proves a binding interaction exists between the coagulant and the pollutant supporting a sorption mechanism.

Without clay, the total aluminium concentration increases to 30 mg l^{-1} before levelling out when the rates of formation and removal of the hydrolysed aluminium precipitate converge. The clay provides binding sites and is removed with the coagulant, yet when no clay is present, and hence

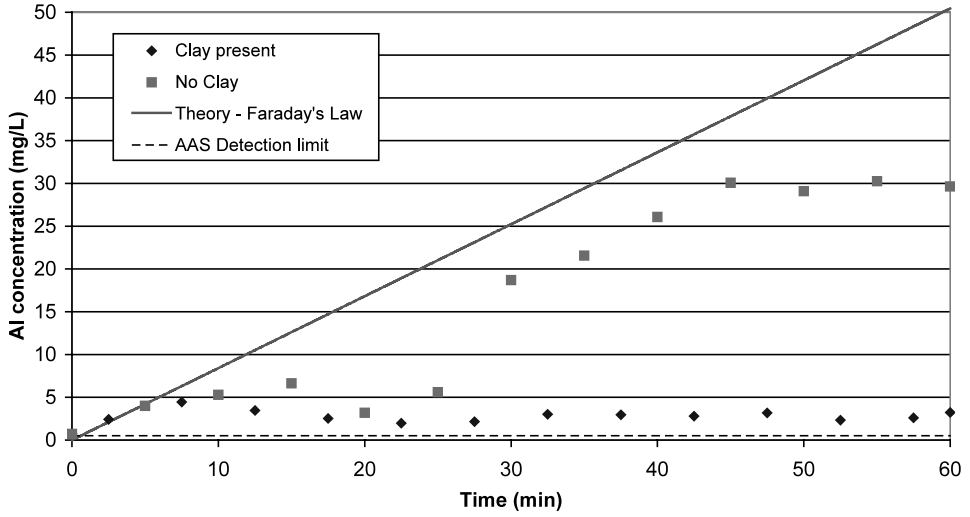

Fig. 11. Total Aluminium concentration for 1 and 0 g l^{-1} clay solution subjected to electrocoagulation at a constant current of 1.0 A.

the absence of binding sites, the added aluminium forms a colloidal suspension of microcrystalline aluminium hydroxide flocs [11]. This contributes to a residual turbidity level, observed during the stable phase and the difference in measured aluminium concentration. Absence of binding sites, that is, the clay pollutant, results in the different behaviour of the electrocoagulation system. Thus the convergence of turbidity levels for the two scenarios considered (with and without clay) is coincidental with the aluminium and clay properties dictating the residual turbidity levels.

3.3. Electrocoagulation — change in current

After the colloidal suspension has been destabilised, effective aggregation requires adequate contact between the coagulant and pollutant particles. Consequently, the transport mechanism is important as this determines the transportation of, including collisions between, particles coagulant and bubbles. Thus the fluid regime clearly has a significant impact on both the flocculation mechanism and the subsequent means of pollutant removal. Hence Table 1 describes flocculation mechanisms and associated transport properties [11].

The current not only determines the coagulant dosage rate but also the bubble production rate and fluid regime (mixing) within the reactor. Hence the collision between particles, floc growth and the potential for material removal, both pollutant and coagulant, by flotation is determined by the current.

Table 1
Flocculation mechanisms and associated fluid regime

Flocculation Mechanism	Transport Mechanism	Forces on particles
Perikinetic flocculation	Brownian fluid motion	Random motion
Orthokinetic flocculation	Laminar flow	Low shear
Turbulent conditions	Fluctuating flows and eddies	High shear
Differential settling	Unequal settling velocities	Gravity

Fig. 12 shows pollutant removal behaviour when current was varied form 0.25–2 A. For all cases, however, regardless of initial value, the pH stabilises within 15 min to somewhere in the range 8.3–8.8. The highest current (2 A) produced the shortest lag (10 min) and the quickest response, with a 90% turbidity reduction occurring between 10 and 15 min. As the current decreased, the length of each electrocoagulation stage increased.

The results of mass balances performed on the electrocoagulation reactor are presented in Table 2. Pollutant loading was constant for all experiments with current being altered. At 0.25 A, 26% of the total pollutant was recovered at the surface after 4 h of operation with the remaining mass recovered as sludge at the reactor base. Conversely, the highest current, 2 A, produced the largest pollutant recovery at the surface (63% of the total). Low current produces low (hydrogen) bubble density, leading to a low upward momentum flux, and thus poor mixing within the reactor-conditions that encourage sedimentation over flotation. As the current is increased, the bubble density and the amount of mixing increase — favouring flotation over sedimentation [7]. Hence, the operational current has a strong influence on the dominant pollutant removal path, that is, flotation (surface) or settling (base) and consequently sludge production.

As noted, the amount of aluminium entering solution can be calculated as a function of time using Faraday's law (Eq. (6)). For example, operation at 1 A for an hour corresponds to a total aluminium dosage of 40 mg-Al l^{-1} for a reactor volume of 6 l. Fig. 13 presents the same electrocoagulation performance data as in Fig. 12, but presented on an equivalent aluminium basis, that is, on the basis of the total amount of aluminium electrochemically added to solution up to a given point in time.

Reactor behaviour is shown to be a strong function of aluminium concentration. However, the order of turbidity reduction has reversed relative to the time-based data. The lower the current, the less aluminium is used to achieve an equivalent turbidity reduction. In addition, the characteristic stages, that is, lag, reactive and stabilising for each current occurs at different

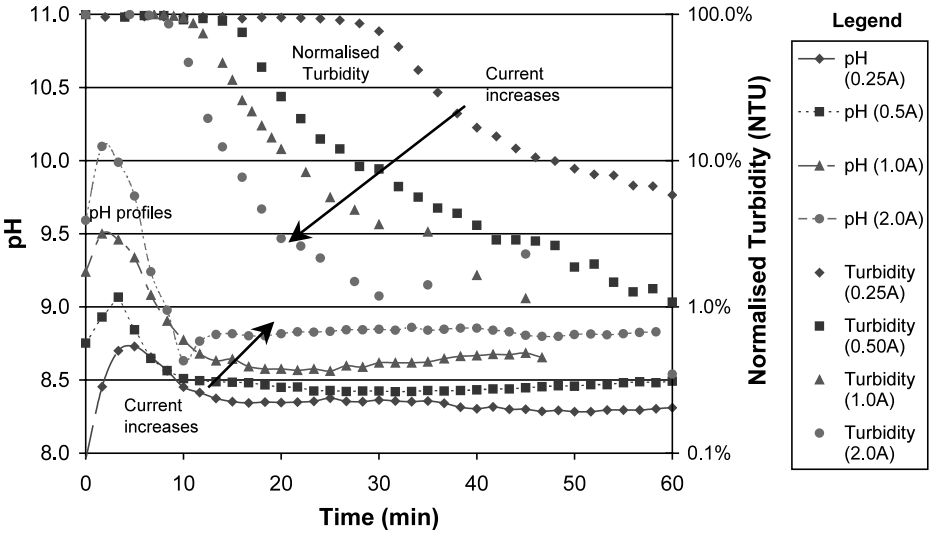

Fig. 12. Normalised turbidity and pH for 1 g l^{-1} clay solution subjected to electrocoagulation at a current of 0.25, 0.5, 1 and 2 A as a function of time.

Table 2
Mass Balance of electrocoagulation reactor. $I = 0.25$, 1.0 and 2.0 A; 1 g l^{-1} clay solution

Current	0.25 A	1.0 A	2.0 A
Clay at surface of reactor	26%	54%	63%
Clay at base of reactor	73%	42%	39%
Error in mass balance	1%	4%	−2%

aluminium levels. Efficiency, defined as aluminium delivered per unit of pollutant removed, appears highest for a current of 0.25 A. As the current increases, the efficiency, on an aluminium basis, decreases.

At high current, the coagulant dosage rate increases resulting in a greater amount of precipitate in the stable stage. Likewise the bubble

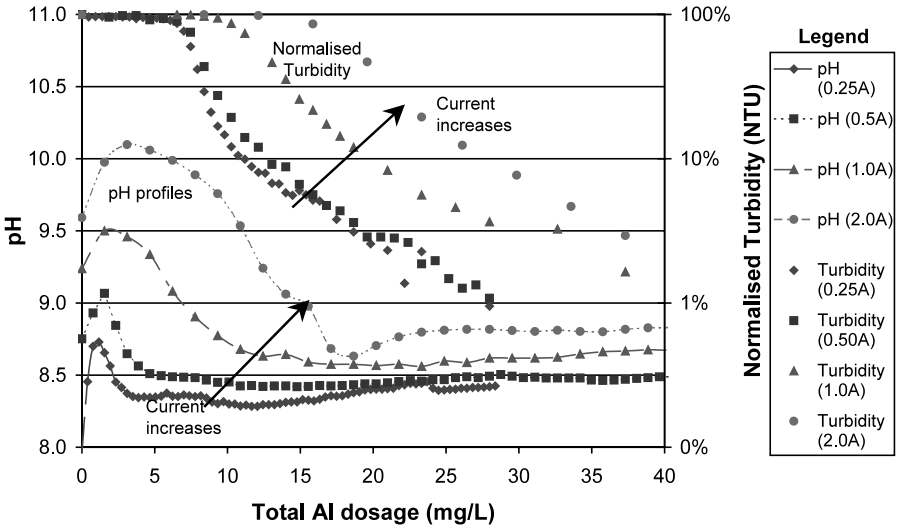

Fig. 13. Normalised turbidity and pH for 1 g l^{-1} clay solution subjected to electrocoagulation at a current of 0.25, 0.5, 1 and 2 A as a function of equivalent aluminium.

density increases resulting in a greater upwards momentum flux and thus faster removal of pollutant and coagulant by flotation [7]. At higher currents, more coagulant (aluminium) is available per unit time but there is a decrease in its residence time in the reactor. Hence there is a reduction in the probability of collision and adhesion between the pollutant and coagulant. This results in the observed decrease in efficiency on an aluminium basis. Consequently the electrocoagulation reactor operational current must be determined by a trade-off between reaction time, aluminium efficiency and desired pollutant path (flotation or settling), in other words, the sludge production.

3.4. Comparison of electro- and chemical coagulation

A direct comparison between electro- and chemical coagulation is not practicable. The systems do not operate on an equivalent basis. In chemical coagulation, coagulant addition is a discrete (shot-fed) event with equilibrium determining aluminium speciation and pH. In electrocoagulation the coagulant addition is a function of current and time. Concentration gradients continually shift as the aluminium electrode corrodes yet the pH stabilised at 8.3–8.8, depending on current (see Fig. 12). Pollutant separation processes are also different with settling the only removal path for chemical coagulant while a combination flotation/settling is employed by electrocoagulation. Thus, it is important to compare turbidity reduction on a more consistent basis.

A new set of chemical coagulation runs were carried out in which the pH was varied by addition of hydrochloric acid or sodium hydroxide solution. The alum dosages chosen for these runs (4 and 20 mg-Al l^{-1}) are significant for chemical dosing because they span the range of optimal turbidity reduction without pH adjustment (see Fig. 5), and for electrocoagulation because they span the stage during which most turbidity reduction occurs. Thereby enabling comparison at comparable pH values and aluminium concentrations. Normalised turbidity response curves for the chemical dosing jar tests at a range of pHs are presented in Fig. 14 and Fig. 15 for 4 and 20 mg-Al l^{-1} alum dosage levels, respectively.

Alum dosing at 4 mg-Al l^{-1} produced average performance and is presented in Fig. 14. A high residual turbidity was observed with the turbidity dropping to 10% of its initial value after settling for 60 min. The best turbidity reduction achieved was at an unaltered (i.e. no acid or base addition) pH of 4.1 where the zeta potential is closest to zero (Fig. 7). As the pH increases, zeta potential moves away from zero indicating an increase in stability of the solution and turbidity removal performance declines. Indeed, under strongly basic conditions (pH $\sim$11.4), settling performance was so poor as to indicate substantial restabilisation of the colloidal clay [17]. This sub-optimal turbidity removal performance is more noticeable in the electrocoagulation results.

Considering the electrocoagulation results in Fig. 13, by 4 mg-Al l^{-1} no turbidity removal has occurred regardless of the current used. Turbidity removal began at 7 mg-Al l^{-1} for 0.25 A, with the concentration necessary for the start of turbidity reduction increasing as the current increases. At 4 mg-Al l^{-1}, the pH was far higher (8.3-10.1) than the optimal (acidic) pH of 4.2 identified for chemical dosing with alum where charge neutralisation was identified as the dominant coagulation mechanism [16]. As the pH increased, zeta potential decreased and performance deteriorated. The two sets of results are, thus, consistent with the lag stage observed in electrocoagulation being characterised by a low coagulant level and a high pH — a combination where both chemical and electro- coagulation are far from optimal.

In the electrocoagulation reactor at 20 mg-Al l^{-1}, pH has levelled out to 8.3–8.8, which is towards the upper end of the range identified by alum dosing (see Fig. 13) as leading to 'good' turbidity reduction. For 2 A, the system is still in the reactive stage at 20 mg-Al l^{-1} with the turbidity still dropping rapidly as the aluminium concentration increases. On an equivalent aluminium basis, efficiency has declined due to the higher bubble production rate resulting in the domination of flotation, as previously discussed. At low current the coagulant release is slow, bubble production low hence gentle agitation

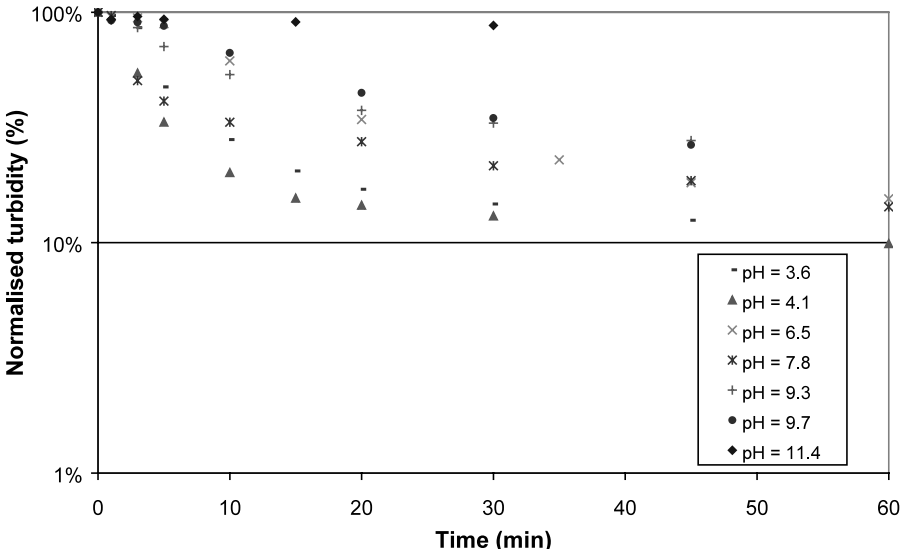

Fig. 14. Normalised turbidity tests for 1 g l^{-1} clay solutions at 4 mg-Al l^{-1} subjected to chemical dosing as a function of time and pH.

favouring removal by settling conditions, which more closely resemble those in chemical coagulation jar tests. Thus a more realistic comparison between chemical and electro- coagulation is at low currents.

The normalised turbidity for alum dosage at 20 mg-Al l^{-1} is presented in Fig. 15. Here, pH adjustment improved turbidity reduction with good performance demonstrated over pH 5.2–9.3, where residual turbidity fell to between 5–7% after 60 min. This region coincides, to a first approximation, to the pH range of 4–8 spanning the isoelectric points identified in chemical coagulation (Fig. 8). Thus implying the clay solution is destabilised, to a certain extent, and coagulation by a sorption mechanism. Outside this range,

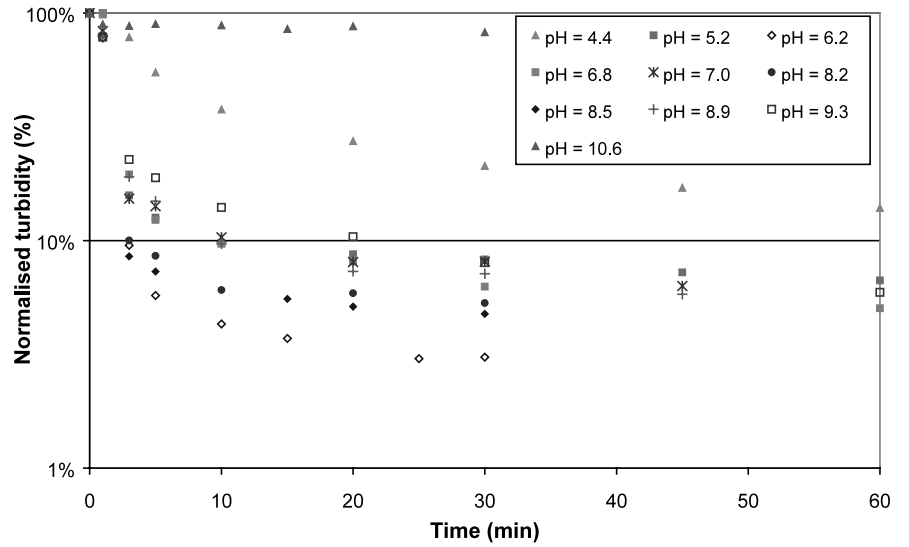

Fig. 15. Normalised turbidity tests for 1 g l^{-1} clay solutions at 20 mg-Al l^{-1} subjected to chemical dosing as a function of time and pH.

however, zeta potential decreased resulting in a stable solution reflected by a decline in turbidity removal performance. At a highly alkaline pH, ~ 10.6, little change in turbidity was observed, due to restabilisation of the colloidal clay and the dominance of the aluminate ion in solution [16,17]. Thus at alum concentration of 20 mg-Al l^{-1} turbidity removal performance is better and occurs over a wider pH range than at 4 mg-Al l^{-1}.

At 20 mg-Al l^{-1} and at low currents (0.25 and 0.5 A) the electrocoagulation system operates in the final (stable) stage. Aluminium hydroxide precipitates removing the remaining clay particles by sweep coagulation, resulting in a small change of turbidity. In comparison to chemical coagulation at 20 mg-Al l^{-1}, the electrocoagulation reactor achieves better pollutant removal (than alum dosing) with normalised turbidity being reduced to about 3% for both 0.25 and 0.5 A. Differences due to bubble density and removal by flotation have been minimised by operating at low currents. The remaining differences between the systems are the presence of the sulphate ion from alum (chemical coagulation) and the reaction time for equivalent aluminium levels (electrocoagulation). The presence of the sulphate anion, SO_4^{2-}(aq), from alum has been suggested to improve sweep coagulation by destabilising positively charged ions (usually hydrolysis products) and adsorption into the Stern layer [11]. In this case it appears electrocoagulation produces a better result than chemical coagulation. Hence the absence of sulphate anions and presence of hydroxyl ions, OH^-(aq), formed at the cathode, appears to improve overall performance. However, to achieve equivalent levels of coagulant dosage on an aluminium basis for 0.25 and 0.5 A, the reactor was operated for 85 and 43 min, respectively. This reaction time has a direct impact the settling time. It appears that operation at 0.25 A has longer time to allow clay pollutant to settle but this is not the case at 0.50 A. Thus it is questionable to the governing influence that has resulted in the better performance of electrocoagulation at 20 mg-Al l^{-1}. A multitude of factors including, coagulant and pollutant type and concentration, dominant removal path (flotation and/or settling), solution pH, zeta potential, aqueous speciation to name a few, must be explored in variety of dimensions, that is, time and space to understand the complexities of electrocoagulation.

4. Conclusions

The dynamic nature of batch electrocoagulation is characterised by lag, reactive and stable stages. During the lag stage, no turbidity reduction occurs while the pH (after an initial increase) begins to stabilise in the range 8.3–8.8. During the reactive stage, the isoelectric point is reached and turbidity decreases rapidly, while in the stable stage turbidity asymptotes out. In the case of clay removal, the colloid is destabilised at a critical aluminium concentration that is dependent on the applied current. The results indicate that a sorption removal mechanism is dominant during the reactive stage. Further turbidity reduction in the stable stage is attributed to pollutant removal by a sweep coagulation mechanism.

The fundamental physical separation processes are different for chemical dosing and electrocoagulation, with settling being the key removal path in the former case. In electrocoagulation, however, the dominant removal path is determined by the applied current. At low currents, settling dominates. As the current increases, so the pollutant fraction that is removed by flotation increases, although the coagulant appears to be used less effectively. Experimental data support the hypothesis that the increased bubble densities associated with higher currents are removing flocs of coagulant from solution.

The mechanism of coagulant delivery is a key difference between chemical dosing and electrocoagulation performance. In the alum dosing studied here, coagulant addition is a discrete event with the system then moving towards an acidic equilibrium. Modification of pH was shown to be able to improve turbidity reduction under some conditions. By contrast, in electrocoagulation the continuous addition of aluminium and hydroxyl ions (with the multi-step hydrolysis of the former) results in a non-equilibrium state. Somewhat surprisingly, however, the system appears stable, at least with respect to pH, during the reactive and

stable stages. The relationship between thermodynamic equilibrium and reaction kinetics, both in the solution and in terms of pollutant removal, are clearly significant for a deeper understanding of electrocoagulation.

References

[1] M. Matteson, L. Regina, R. Glenn, N. Kukunoor, W. Waits, E. Clayfield, Electrocoagulation and separation of aqueous suspensions of ultrafine particles, Colloids and Surfaces A: Physicochemical and Engineering Aspects 104 (1) (1995) 101–109.
[2] E.A. Vik, D.A. Carlson, A.S. Eikum, E.T. Gjessing, Electrocoagulation of potable water, Water Research 18 (11) (1984) 1355–1360.
[3] P. Holt, G. Barton, C. Mitchell, Electrocoagulation as a wastewater treatment, The Third Annual Australian Environmental Engineering Research Event, 1999, M:41–46.
[4] N.P. Barkley, C.W. Farrell, T.W. Gardner-Clayson, Alternating current electrocoagulation for superfund site remediation Air and Waste 43 (5) (1993) 784–789.
[5] N. Mameri, A.R. Yeddou, H. Lounici, D. Belhocine, H. Grib, B. Bariou, Defluoridation of Septentrional Sahara water of North Africa by electrocoagulation process using bipolar aluminium electrodes, Water Research 32 (5) (1998) 1604–1612.
[6] M.F. Pouet, A. Grasmick, Urban wastewater treatment by electrocoagulation and flotation', Water Science and Technology 31 (3-4) (1995) 275–283.
[7] P.K. Holt, G.W. Barton, C.A. Mitchell, A step forward to understanding electrocoagulation, characterisation of pollutant's fate, Sixth World Congress of Chemical Engineering, Melbourne, 2001.
[8] J. Lyklema, in: K.J. Ives (Ed.), The Scientific Basis of Flocculation, Sijthoff and Noordhoff International Publishers, Apphen aan den Rijn, The Netherlands, 1978.
[9] D.N. Thomas, S.J. Judd, N. Fawcett, Flocculation Modelling: A review, Water Research 33 (7) (1999) 1579–1592.
[10] R.J. Hunter, Introduction to Modern Colloid Science, Oxford University Press, Oxford, 1993.
[11] R.D. Letterman, A. Amirtharajah, C.R. O'Melia, Coagulation and flocculation in water quality and treatment, in: R.D. Letterman (Ed.), A Handbook of Community Water Supplies, Fifth, AWWA, McGraw-Hill, New York, 1999.
[12] B.V. Deryaguin, L.D. Landau, A theory of the stability of strongly charged lyophobic sols and so the adhesion of strongly charged particles in solutions of electrolytes, Acta Physicochim, USSR 14 (1941) 633.
[13] E.J.W. Verwey, J.T.G. Overbeek, Theory of the Stability of Lyphobic Colloids, Elsevier, Amsterdam, 1948.
[14] W.J. Eilbeck, G. Mattock, Chemical Processes in Waste Water Treatment, Ellis Horwood Limited, Chichester, 1987.
[15] G. Sposito, The Environmental chemistry of aluminum, Second, CRC Press Ltd, Florida, 1996.
[16] W. Stumm, J.J. Morgan, Chemical aspects of coagulation, Journal American Water Works Association 54 (8) (1962) 971–992.
[17] W. Stumm, C.R. O'Melia, Stoichiometry of coagulation Journal American Water Works Association 60 (5) (1968) 514–539.
[18] A. Amirtharajah, K.M. Mills, Rapid-mix design for mechanisms of alum coagulation, Journal American Water Works Association 74 (4) (1982) 210–216.
[19] T.M. Riddick, Role of the zeta potential in coagulation involving hydrous oxides, Tappi 47 (1) (1964) 171A–179.
[20] J. Bratby, Coagulation and Flocculation with an Emphasis on Water and Wastewater Treatment, Uplands Press, Croydon, 1980.